Laser-driven ion acceleration enhancement using silicon nitride plasma shutter

M. Matys [1,2], M. Kecova [1], M. Kucharik [1,2], J. Nikl [1,2], S. V. Bulanov [1,3], M. Jirka [1,2], P. Janecka [1], J. Psikal [1,2], G. Korn [1], J. Grosz [1] and O. Klimo [1,2]

[1] *ELI Beamlines Centre, IoP, Czech Academy of Sciences, Dolni Brezany ,Czech Republic*

[2] *FNSPE, Czech Technical University in Prague, Prague, Czech Republic*

[3] *Kansai Photon Science Institute - QST, Kyoto, Japan*

A plasma shutter is usually a thin solid foil or membrane which is placed in front of the main target in the laser-target interaction. The laser pulse with its accompanying prepulses [1] then needs to burn through the plasma shutter before the main interaction with the target, as can be seen in the scheme in Fig. 1. The interaction of the laser pulse with the plasma shutter then leads to the modification of the intensity profile (formation of a steep-rising front and intensity increase) and mitigation of its prepulses. The concept was proposed in theory and proved in various experiments and simulations [2–6]. The formation of a steep-front laser pulse can be utilized to enable the development of long-wavelength instabilities induced by the special target geometry (double-layer with corrugated interface) for the generation of collimated high energy ion beams as was demonstrated in Ref. [7]. Another utilization of the steep-front laser pulse is to enhance photon emission from under-dense targets as was shown in Ref. [8].

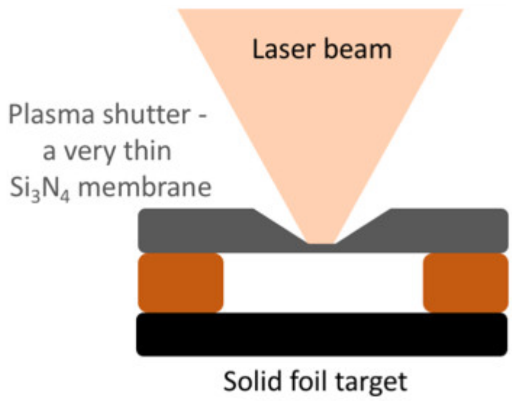

Figure 1: *Scheme of the plasma shutter application in the laser - solid target interaction.*

In this work, we focus on the application of local intensity increase of the laser pulse transmitted through the ultra-thin plasma shutter, mainly in the laser-driven heavy ion acceleration. We demonstrated with the help of fully 3D particle-in-cell (PIC) simulation of PW-class laser interaction with silicon nitride (Si_3N_4) plasma shutter, that the intensity can be increased by the factor of 7, which corresponds to our theoretical estimations [9]. The silver target is then added into the simulations at the position around the local maxima of the transmitted laser pulse. This leads to the increase of maximal silver ion energy by 42.2 % compared to the simulation without the plasma shutter [10]. A scheme utilizing double-shutter configuration (the first one filtering out the prepulses and the second one shaping the main pulse) is also proposed [10]. The prepulses are taken into account in the investigation of this scheme via a combination of the PIC and hydrodynamic simulations done in the codes EPOCH [11] and PALE [12].

The visualization of the 3D PIC simulation with the plasma shutter and silver target is shown in Fig. 2. The simulation box contains a fully ionized silicon nitride plasma shutter of electron density $n_e = 835\ n_c$ and thickness $d = 20$ nm, a partially ionized silver target of $n_e = 2100\ n_c$ and $d = 20$ nm, where the critical density corresponds to $n_c \approx 1.115 \times 10^{21}$ cm^{-3} in our case. The silver target is not completely ionized, which is in agreement with the experiments of a similar type of laser with a silver target [13]. For simplicity, the charge number $Z = 40$ and mass number $A = 108$ are used in our simulations.

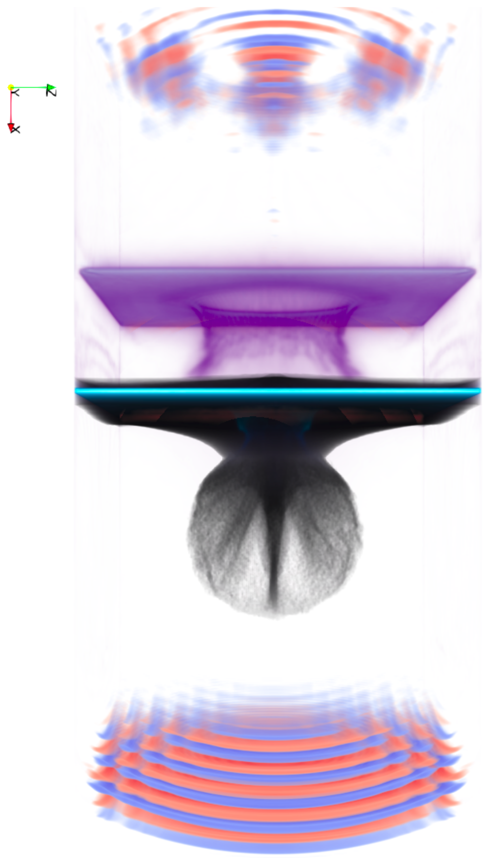

Figure 2: *Visualization of our 3D simulation of plasma shutter (purple), main target (light blue for the foil and black for accelerated particles) and reflected/transmitted laser pulse (red/blue for +/– electric field).*

The incoming laser pulse is linearly polarized, has a Gaussian spatial profile with the full width at half maximum (FWHM) equal to 3 λ. The temporal profile has a $\sin^2$ shape in intensity and beam duration is 64 fs. The pulse roughly corresponds to a 30 fs long 1 PW laser pulse with a Gaussian shape. The radiation wavelength is $\lambda = 1\ \mu$m and the peak intensity is $I_{\max} = 1 \times 10^{22}$ W/cm^2, thus yielding dimensionless amplitude $a_0 = eE_0/m_e\omega c \approx 0.85\sqrt{I\,[10^{18}\mathrm{W/cm^2}]\,\lambda^2\,[\mu\mathrm{m}]} \approx 85$. Here, E_0 is the electric field amplitude, ε_0 is permittivity of vacuum, ω is laser angular frequency, m_e and e are electron mass and charge, respectively, and c is speed of light in vacuum.

As can be seen in Fig. 2, the laser pulse (red and blue) incoming from above, partially reflects and partially burns through the plasma shutter (purple), modifying its intensity profile. The transmitted part of the laser pulse then interacts with the silver target (light blue for the foil and black for the accelerated particles), gradually making it (relativistically) transparent and subsequently burning through it. The acceleration is then dominated by a hybrid RPA-TNSA scheme enhanced by the onset of relativistic induced transparency [14].

In Fig. 3, the silver ion energy spectra are shown at the end of the simulation (at time $t = 70\ T$), when the acceleration in both cases already ended. Maximal energy increases from 109 MeV/A to 155 MeV/A (by 42.2 %) when the plasma shutter is included in the simulation. The inset in Fig. 3 shows the corresponding 2D simulations, they are also compared to the double-shutter scheme. Firstly, the 2D hydrodynamic simulation with a prepulse of intensity $I = 10^{12}\ \mathrm{W/cm^2}$ and duration of 125 ps and plasma shutter was performed. The resulting 2D density profile of the first (expanded) plasma shutter is then imported into a 2D PIC simulation containing also the second plasma shutter with the step-like density profile and the silver target. This scheme also results in a significant energy increase compared to the case without any plasma shutter, as can be seen in the inset of Fig. 3. Note that the maximal silver ion energy in the case without any shutter may be significantly lower than in our simulation if the target would be pre-expanded by the same prepulse [3].

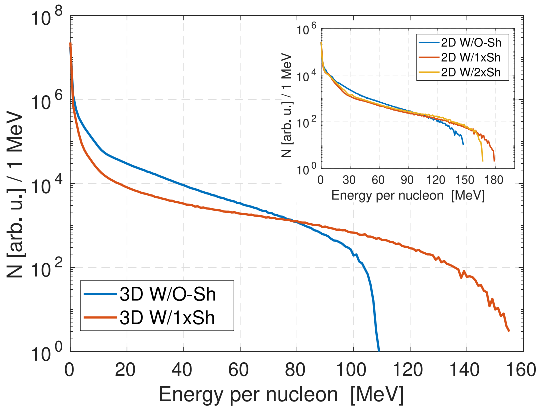

Figure 3: *Silver ion energy spectra in the 3D cases without and with the plasma shutter (corresponding 2D cases in the inset).*

In the frame of this research, we obtain huge volumetric data. Therefore, we collaborate with our VBL team at ELI Beamlines Centre on the visualizations. Down-sampled simulation data were converted into .h5 files and visualized using ParaView [15], as in Fig. 2. The data have been also presented in our custom-made web-based interactive 3D application [16], as can be seen in Fig. 4. The application provides real-time viewing of prepared time frames with features like rotation and zoom. The application runs in a regular web browser and also utilizes a VR (virtual reality) mode via a headset, which provides a great way for the popularization of science for the general public. The color maps can be changed directly in the application. A different color map version of Fig. 4 can be found in [10].

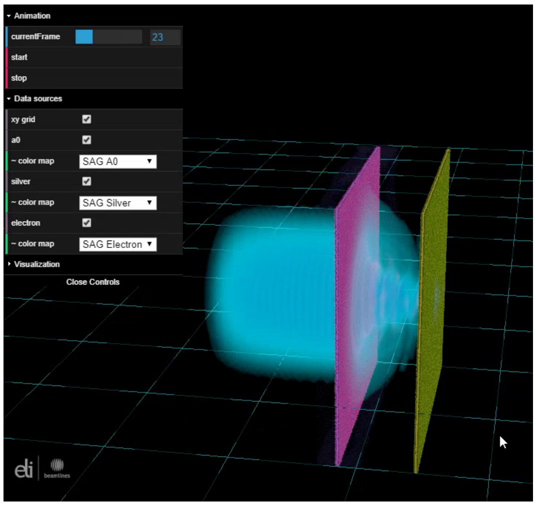

Figure 4: *Visualization of our 3D results in the custom-made web-based application. The application is interactive, enabling rotation, zoom and other functions via mouse clicking. Virtual Reality mode can be used via headset.*

In conclusion, the application of the silicon nitride membrane as a plasma shutter in interaction with a PW-class laser pulse for ion acceleration was demonstrated. Application of the plasma shutter resulted in the increase of maximal silver ion energy by 42.2 % compared to the case without the plasma shutter. The scheme with a double-plasma shutter was proposed, which also provided a significant increase of maximal silver ion energy.

Our work is supported by projects: High Field Initiative (CZ.02.1.01/0.0/0.0/15_003/0000449) - European Regional Development Fund; Plasma optics for ultra-intense laser physics experiments (18-09560S) - Czech Science Foundation; Center of Advanced Applied Natural Sciences (CZ.02.1.01/0.0/0.0/16_019/0000778) - Ministry of Education, Youth and Sports; ELI Beamlines: International Center of Excelence (LQ1606) - Ministry of Education, Youth and Sports, the National Program of Sustainability II; The Photon and Neutron Open Science Cloud - PaNOSC (No. 823852). The computer resources for simulations were provided by the Large Infrastructures for Research, Experimental Development and Innovations project "IT4Innovations National Supercomputing Center - LM2015070". Data storage was supplied by the project "e-Infrastruktura CZ" (e-INFRA LM2018140) provided within the program Projects of Large Research, Development and Innovations Infrastructures. The support of the Grant Agency of the Czech Technical University in Prague is appreciated, grants no. SGS19/192/OHK4/3T/14 and SGS19/191/OHK4/3T/14.

References

[1] G. A. Mourou, T. Tajima, and S. V. Bulanov, Reviews of Modern Physics **78**, 309 (2006).

[2] V. A. Vshivkov, N. M. Naumova, F. Pegoraro and S. V. Bulanov, Physics of Plasmas **5**, 2727 (1998).

[3] S. A. Reed, T. Matsuoka, S. Bulanov, et al., Applied Physics Letters **94**, 201117 (2009).

[4] S. Palaniyappan, B. M. Hegelich, H. C. Wu, et al., Nature Physics **8**, 763-769 (2012).

[5] W. Q. Wei, X. H. Yuan, Y. Fang, et al., Physics of Plasmas **24**, 113111 (2017).

[6] M. Matys, O. Klimo, J. Psikal and S. V. Bulanov, Europhysics conference abstracts, **42A**, P4.2031 (2018).

[7] M. Matys, K. Nishihara, M. Kecova, et al., High Energy Density Physics **36**, 100844 (2020).

[8] M. Jirka, O. Klimo, Y.-J. Gu and S. Weber, Scientific Reports **10**, 8887 (2020).

[9] M. Jirka, M. Matys and O. Klimo, arXiv:2105.06106 (2021).

[10] M. Matys, S. V. Bulanov, M. Kecova, et al., Proc. SPIE **11779**, Laser Acceleration of Electrons, Protons, and Ions VI, 117790Q (2021).

[11] T. D. Arber, K. Bennett, C. S. Brady, et al., Plasma Physics and Controlled Fusion **57**, 113001 (2015).

[12] R. Liska, M. Kucharik, J. Limpouch, et al., Finite Volumes for Complex Applications VI Problems & Perspectives **978-3-642-20671-9**, 857-873, Springer, Berlin (2011).

[13] M. Nishiuchi, N. P. Dover, M. Hata, et al., Physical Review Research **2**, 033081 (2020).

[14] A. Higginson, R. J. Gray, M. King, et al., Nature Communications **9**, 724 (2018).

[15] J. Ahrens, B. Geveci and C. Law, Visualization Handbook **978-0-12-387582-2**, 717-731, Elsevier Inc. (2005).

[16] M. Danielova, P. Janecka, J. Grosz and A. Holy, EuroVis 2019 - Posters **978-3-03868-088-8**, 57-59, The Eurographics Association (2019).